

| | | | | | |
|---|-------------------|-------------------------------|----------------------------------|---|---|
| REPORT DOCUMENTATION PAGE | | | Form Approved OMB NO. 0704-0188 | | |
| <p>The public reporting burden for this collection of information is estimated to average 1 hour per response, including the time for reviewing instructions, searching existing data sources, gathering and maintaining the data needed, and completing and reviewing the collection of information. Send comments regarding this burden estimate or any other aspect of this collection of information, including suggestions for reducing this burden, to Washington Headquarters Services, Directorate for Information Operations and Reports, 1215 Jefferson Davis Highway, Suite 1204, Arlington VA, 22202-4302. Respondents should be aware that notwithstanding any other provision of law, no person shall be subject to any penalty for failing to comply with a collection of information if it does not display a currently valid OMB control number.</p> <p>PLEASE DO NOT RETURN YOUR FORM TO THE ABOVE ADDRESS.</p> | | | | | |
| 1. REPORT DATE (DD-MM-YYYY) | | 2. REPORT TYPE New Reprint | | 3. DATES COVERED (From - To) - | |
| 4. TITLE AND SUBTITLE Synthesizing aluminum particles towards controlling electrostatic discharge ignition sensitivity | | | | 5a. CONTRACT NUMBER W911NF-11-1-0439 | |
| | | | | 5b. GRANT NUMBER | |
| | | | | 5c. PROGRAM ELEMENT NUMBER 611102 | |
| 6. AUTHORS Eric S. Collins, Jeffery P. Gesner, Michelle L. Pantoya, Michael A. Daniels | | | | 5d. PROJECT NUMBER | |
| | | | | 5e. TASK NUMBER | |
| | | | | 5f. WORK UNIT NUMBER | |
| 7. PERFORMING ORGANIZATION NAMES AND ADDRESSES Texas Technical University Box 41035 349 Admin Bldg Lubbock, TX 79409 -1035 | | | | 8. PERFORMING ORGANIZATION REPORT NUMBER | |
| 9. SPONSORING/MONITORING AGENCY NAME(S) AND ADDRESS (ES) U.S. Army Research Office P.O. Box 12211 Research Triangle Park, NC 27709-2211 | | | | 10. SPONSOR/MONITOR'S ACRONYM(S) ARO | |
| | | | | 11. SPONSOR/MONITOR'S REPORT NUMBER(S) 58857-EG.43 | |
| 12. DISTRIBUTION AVAILABILITY STATEMENT Approved for public release; distribution is unlimited. | | | | | |
| 13. SUPPLEMENTARY NOTES The views, opinions and/or findings contained in this report are those of the author(s) and should not be construed as an official Department of the Army position, policy or decision, unless so designated by other documentation. | | | | | |
| 14. ABSTRACT Aluminum particles were synthesized with shell thicknesses ranging from 2.7 to 8.3nm and a constant diameter of 95nm. These fuel particles were combined with molybdenum trioxide particles and the electrostatic discharge (ESD) sensitivity of the mixture was measured. Results show ignition delay increased as the alumina shell thickness increased. These results correlated with electrical resistivity measurements of the mixture which increased with alumina concentration. A model was developed using COMSOL for ignition of a single Al particle. The ignition delay in the model was consistent with the experimental results suggesting that the primary ESD ignition | | | | | |
| 15. SUBJECT TERMS ignition, electrostatic discharge, aluminum, aluminum ignition, ESD safety | | | | | |
| 16. SECURITY CLASSIFICATION OF: | | | 17. LIMITATION OF ABSTRACT UU | 15. NUMBER OF PAGES | 19a. NAME OF RESPONSIBLE PERSON Michelle Pantoya |
| a. REPORT UU | b. ABSTRACT UU | c. THIS PAGE UU | | | 19b. TELEPHONE NUMBER 806-742-3563 |

Report Title

Synthesizing aluminum particles towards controlling electrostatic discharge ignition sensitivity

ABSTRACT

Aluminum particles were synthesized with shell thicknesses ranging from 2.7 to 8.3nm and a constant diameter of 95nm. These fuel particles were combined with molybdenum trioxide particles and the electrostatic discharge (ESD) sensitivity of the mixture was measured. Results show ignition delay increased as the alumina shell thickness increased. These results correlated with electrical resistivity measurements of the mixture which increased with alumina concentration. A model was developed using COMSOL for ignition of a single Al particle. The ignition delay in the model was consistent with the experimental results suggesting that the primary ESD ignition mechanism is joule heating.

REPORT DOCUMENTATION PAGE (SF298) (Continuation Sheet)

Continuation for Block 13

ARO Report Number 58857.43-EG

Synthesizing aluminum particles towards contro...

Block 13: Supplementary Note

© 2014 . Published in Journal of Electrostatics, Vol. Ed. 0 72, (1) (2014), (, (1). DoD Components reserve a royalty-free, nonexclusive and irrevocable right to reproduce, publish, or otherwise use the work for Federal purposes, and to authorize others to do so (DODGARS §32.36). The views, opinions and/or findings contained in this report are those of the author(s) and should not be construed as an official Department of the Army position, policy or decision, unless so designated by other documentation.

Approved for public release; distribution is unlimited.



Contents lists available at ScienceDirect

Journal of Electrostatics

journal homepage: www.elsevier.com/locate/elstat

Synthesizing aluminum particles towards controlling electrostatic discharge ignition sensitivity

Eric S. Collins^a, Jeffery P. Gesner^a, Michelle L. Pantoya^{a,*}, Michael A. Daniels^b^a Department of Mechanical Engineering, Texas Tech University, Lubbock, TX 79409, USA^b Idaho National Laboratory, PO Box 1625, Idaho Falls, ID 83415, USA

ARTICLE INFO

Article history:

Received 9 August 2013

Received in revised form

21 October 2013

Accepted 1 November 2013

Available online 21 November 2013

Keywords:

Aluminum oxidation

Joule heating

Electrostatic discharge

Energetic materials

Ignition delay

Electrical conductivity

ABSTRACT

Aluminum particles were synthesized with shell thicknesses ranging from 2.7 to 8.3 nm and a constant diameter of 95 nm. These fuel particles were combined with molybdenum trioxide particles and the electrostatic discharge (ESD) sensitivity of the mixture was measured. Results show ignition delay increased as the alumina shell thickness increased. These results correlated with electrical resistivity measurements of the mixture which increased with alumina concentration. A model was developed using COMSOL for ignition of a single Al particle. The ignition delay in the model was consistent with the experimental results suggesting that the primary ESD ignition mechanism is joule heating.

© 2013 Elsevier B.V. All rights reserved.

1. Introduction

Composite energetic materials (CEM) are defined here as mixtures of aluminum (Al) fuel and metal oxide particles, that ignite to produce exothermic chemical energy. With the advent of nano technology, nano Al fuel particles have shown heightened reactivity compared to their micron scale counterparts [1–3]. Safely handling these powder mixtures requires a thorough understanding of their electrostatic ignition sensitivity yet very few studies on electrostatic discharge (ESD) ignition have been reported in the literature [4–6].

Most ESD ignition research is performed for the discharge of electric energy into a sample rather than by pouring induced inter particle transport (e.g., electrostatic sensitivity that can occur from pouring a powder sample). An interesting finding from studying the literature on electrostatic ignition of powders is that a paradox exists regarding the electrical properties of the powder and the corresponding electrostatic ignition behavior. Glor [7] studied dust particles that had accumulated a charge through inter particle transport. He found that as the powder's electrical conductivity decreased, so does the minimum ignition energy. In other words,

materials with a decreased conductivity are more readily ignited by ESD [7]. In contrast, Foley et al.'s [8] study on Al–CuO showed that increasing electrical conductivity using additives actually decreased the minimum ignition energy of the mixture. A striking difference in these two studies is the way in which the electrical stimuli were introduced to the sample. For Glor [7] electrostatic charge accumulated within the sample, while in Foley et al. [8] the electrostatic charge was discharged into the sample. This paradox poses new research questions that have potential for impactful development in this field.

As a first step, we examined electrostatic discharge (ESD) ignition sensitivity of nine different CEM formulations, limiting the study to only micron Al inclusion [6]. The results showed that at the highest setting on the ESD apparatus (i.e., which corresponded to 100 mJ), only Al–CuO ignited and its corresponding electrical conductivity was measured to be two orders of magnitude above the next mixture, Al–MoO₃ which did not ignite (i.e., 1246 compared with 40 nS/m, respectively). This was the first study to correlate electrical conductivity to ESD ignition sensitivity in energetic materials [6].

The influence of alumina in ESD ignition sensitivity was further studied in Ref. [9]. Specifically, Weir et al. [9] examined the electrical conductance and ESD ignition sensitivity of aluminum and molybdenum trioxide (Al + MoO₃) with varying Al particle size ranging from nano to micron scales. The results showed that as

* Corresponding author. Tel.: +1 806 742 3563; fax: +1 806 742 3451.
E-mail address: mpantoya@gmail.com (M.L. Pantoya).

particle diameter decreased (and alumina concentration increased) the electrical conductance increased by 7 orders of magnitude and minimum ignition energy required for ESD ignition reduced accordingly. On the other hand, discretely added alumina particles significantly reduce the mixtures electrical conductivity, desensitizing the mixture to ESD ignition. This study revealed that the alumina shell may play a significant role in spurring ignition in Al + MoO₃ by accumulating charge and acting as a capacitive network, in contrast to discretely added alumina particles.

The objective of this work is to understand how the electrical conductivity and ESD ignition sensitivity of Al + MoO₃ varies as a function of the thickness of the alumina passivation shell surrounding the Al particles. To accomplish this objective, nano scale Al particles were synthesized with varying shell thicknesses and combined with nano scale MoO₃ particles. The mixture was further studied for electrical conductivity measurements and ESD ignition sensitivity quantified in terms of ignition delay time.

2. Experimental

The Al particles were supplied by Sigma Aldrich and had an average particle diameter of 95 nm. The MoO₃ particles were purchased from Nanostructured and Amorphous Materials Inc. and had an average platelet size of 380 nm. The Al particles were oxidized in an isothermal oven to increase the thickness of the Al₂O₃ shell; thereby synthesizing particles with controlled shell thicknesses. It is noted that the overall particle diameter does not change, such that the shell thickness grows at the interface of aluminum and alumina and as alumina concentration increases, aluminum correspondingly decreases.

2.1. Material synthesis and preparation

A thermogravimetric analyzer (TGA), model STA 409 PC by Netzsch, was used to observe the weight gain of Al particles as the Al oxidized to Al₂O₃. During oxidation in the TGA, 11.48 mg of Al powder was held in a platinum crucible while the temperature increased at a rate of 40 °C per minute in a controlled environment of ultra high purity oxygen. The oven continued to heat until 480 °C, a temperature that provided reasonable reaction rates where oxidation and shell growth was observed. The Al sample remained in the isothermal environment for 180 min as the mass gain was monitored. The precision of the change in mass of the sample in the TGA had a variance of 0.001 mg. This data was used to control oxide shell growth on larger quantities of aluminum powder.

A Neytech Qex oven was used to oxidize Al particles in an isothermal oxygen environment. Ultra high purity oxygen was purged in the oven chamber at a flow rate of 180 cm³/min for 10 min. This procedure ensured that the volume was flushed five times and had a statistical purity of 99% of oxygen in the oven chamber. The Qex oven was set to have a temperature ramp rate of 200 °C/min and a temperature of 480 °C. The settings were programmed in the oven for automated control and repeatability between oxidation procedures. Six samples of 0.9 g of Al powder were prepared for each oxidation cycle. Once the chamber was purged and the temperature of 480 °C was reached, the Al powder remained in the oven for various durations ranging from 8 to 150 min. This variable oxidation time provided different alumina shell thicknesses.

A transmission electron microscope (TEM), model Jeol JEM 2100, was used to examine the Al particles and measure the thickness of the alumina shell with Gatan image analysis software to measure the thickness of the alumina shell. Thickness measurements were taken from at least three different locations on

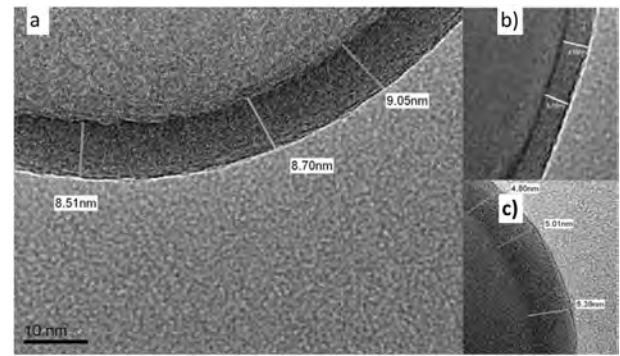


Fig. 1. TEM images of the alumina shell after oxidation times of a) 150 min, b) 8 min, and c) 30 min.

several Al particles. Fig. 1 shows three representative images of the Al particles taken from the TEM.

The percent of active Al by weight (Y) was calculated using Eq. (1),

$$\frac{R^3}{(R - \delta)^3} = \frac{\rho_m}{\rho_{mo}} \left(\frac{1}{Y} - 1 \right) + 1 \quad (1)$$

where R is the average particle radius, δ is the Al₂O₃ shell thickness, and ρ is the density of the metal (m) and metal oxide (mo). The average shell thickness and the percent of active Al content are listed in Table 1 for all treated Al powders.

The Al + MoO₃ mixtures were prepared to an equivalence ratio of 1.0, corresponding to stoichiometric conditions. Details of this mixing procedure are reported in Ref. [10].

2.2. Experimental setup

An acrylic channel was loaded with 58 mg of the powder, which was pressed into a pellet within the channel. The pellet occupied a volume of 31 mm³ and had a bulk density of 1.89 g/cm³. The bulk density of the pellet was calculated to be 50% of the theoretical maximum density (TMD). Two copper electrodes were positioned to cover the openings in the channel such that the tips of the electrodes were in contact with the surface of the pellet as shown in Fig. 2. A voltage potential was applied to the electrodes and when greater than the dielectric strength of the pellet material, a spark was generated which ignited the pellet. The voltage source used in these experiments was an electrostatic discharge (ESD) tester that is a human body model developed by Franklin Applied Physics [6]. A human body model transfers charge from a capacitor (human) to another object. The range of voltage output is 1–10 kV which is stored in a 0.002 μ F capacitor producing up to 100 mJ of energy.

A current monitor, model 2878 from Pearson Electronics, was used to measure the electric charge released by the ESD tester. A

Table 1
Thickness of Al₂O₃ shell and weight percent active Al content for all oxidized Al particles.

| Oxidation time (min) | Al ₂ O ₃ thickness (nm) | Wt % active Al |
|----------------------|---|----------------|
| 0 | 2.7 | 78.1 |
| 8 | 3.3 | 73.9 |
| 15 | 4.5 | 66.3 |
| 30 | 4.6 | 65.7 |
| 60 | 5.7 | 59.4 |
| 90 | 6.7 | 54.2 |
| 150 | 8.3 | 46.7 |

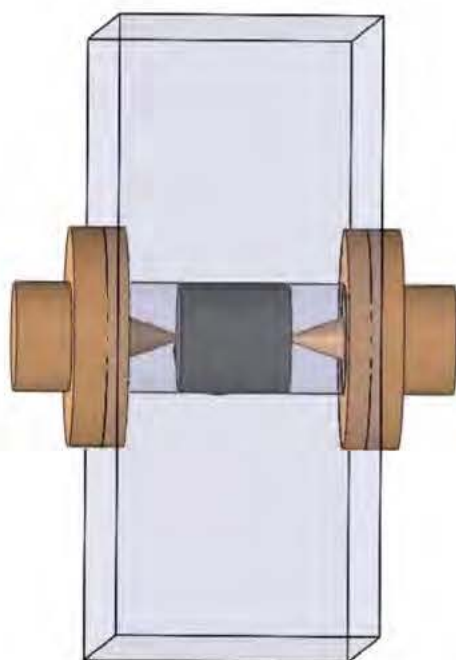


Fig. 2. Electrodes in contact with the pellet in the acrylic channel.

high voltage probe, model P6015A from Tektronix, reduced the voltage 1000 times, enabling the use of oscilloscopes to record the voltage output. Ignition delay time was measured as the length of time between the spark and the instant that luminosity produced a slope of ten, which was the maximum slope observed for all the tests, and detected using a photo detector; model DET210 from Thorlabs (see Fig. 3). The ignition energy was determined from the simultaneous current and voltage measurements.

3. Results

3.1. Ignition delay

As the voltage potential between the two electrodes increased beyond the electric field strength of the medium, a spark bridged the electrode gap and ignited the CEM. Fig. 4 is a good representation of the voltage, current, and luminosity for all tests. As the spark bridged the electrode gap, the voltage decreased and the current increased as shown in Fig. 4a. The length of time between the spark and the instant that luminosity produced a slope of ten

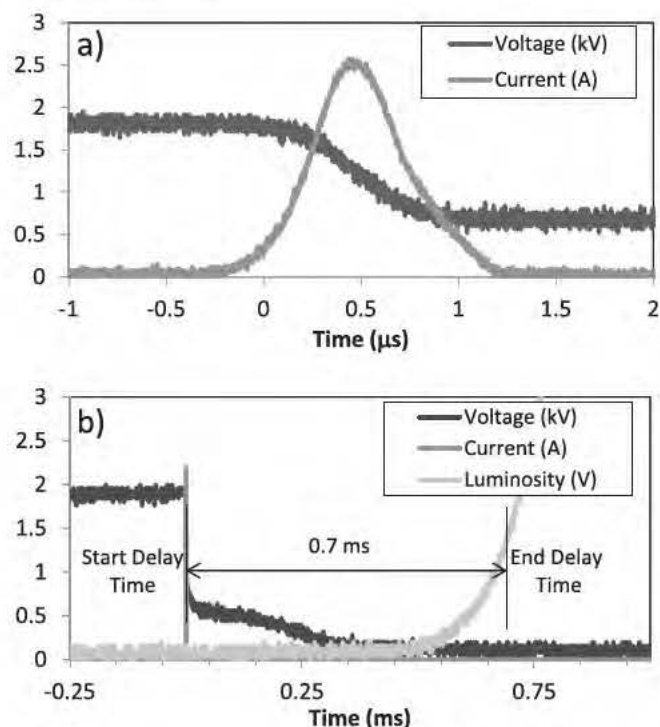


Fig. 4. Voltage, current, and luminosity depicting time delay for Al + MoO₃.

(Fig. 4b) (i.e., corresponding to the maximum slope observed for all the tests) was recorded as the ignition delay for the reaction.

The ignition time delay tests were conducted for CEM mixtures containing each batch of oxidized Al powder identified in Table 1 combined with MoO₃. Three samples were tested for each Al powder with varied shell thickness and the ignition time delay is shown in Fig. 5.

All CEMs were deemed ESD ignition sensitive because all ignited below the maximum energy threshold of 100 mJ supplied by the ESD apparatus. The thinner shelled Al powders experienced the fastest ignition. Ignition delay increased as the Al₂O₃ shell thickness increased. The voltage required to ignite the powders also increased as the Al₂O₃ shell thickness increased (Fig. 6).

3.2. Joule heating of an aluminum particle

The joule heating of a single Al particle was modeled using COMSOL Multiphysics. The equation used for calculating joule heating is the time dependent energy equation for incompressible flow as shown in Eq. (2).

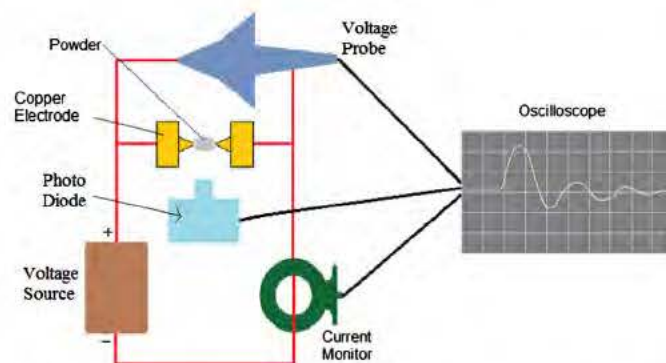


Fig. 3. Electrical circuit used to monitor voltage and current and measure time delay of the reaction.

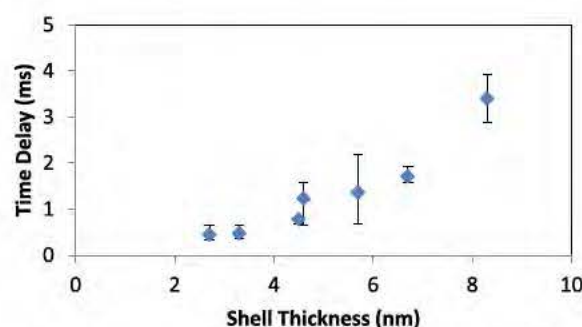


Fig. 5. Ignition time delay for Al + MoO₃ reactions with varying alumina shell thicknesses.

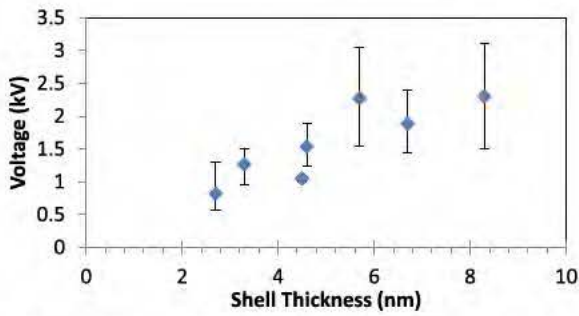


Fig. 6. Ignition voltage for Al + MoO₃ reactions with varying alumina shell thicknesses.

$$\rho C_p \frac{\partial T}{\partial t} + \rho C_p \mathbf{u} \cdot \nabla T = \nabla \cdot (k \nabla T) + \mathbf{J} \cdot \mathbf{E} \quad (2)$$

In Eq. (2), ρ is the density, C_p is the specific heat, T is temperature, t is time, \mathbf{u} is a velocity vector, \mathbf{J} is the current density, and \mathbf{E} is the electric field strength. A single Al particle was modeled and assumed to have a contact point with another particle on its top, bottom, front, back, left, and right surfaces. A current of 1 Amp entered the Al particle at one contact point while the rest of the contact points were held at ground potential. In the model, the initial temperature of the Al particle was 20 °C and an initial electric potential was 0 V. Because convective cooling was neglected in the model due to the fast ignition of the particle, the boundary was insulated thermally. The spherical Al particle was assumed to have a solid Al core with an axisymmetric temperature distribution. The model also assumes homogeneous metals within the particle when in reality, the metals are not homogeneous and contain impurities and cracks.

The model results for transient heating of an Al particle with an Al₂O₃ shell thickness of 2.7 nm are shown in Fig. 7. As current travels through a single particle, temperature quickly increased with time. Since the melting temperatures of the fuel and oxide are similar, 933 and 1068 K respectively, ignition of the particle was assumed to occur at the melting temperature of Al [11] and the model predicts ignition times for these conditions to range from 3.0 to 5.0 ns (Fig. 7). Note that the modeled ignition time is significantly less than the experimentally measured ignition time (Fig. 5). The main reason for this difference is that the model predicts ignition delay for a single particle whereas in the experiments, the delay is measured for a macroscopic collection of particles. The heat transfer among neighboring particles within the random media of the reactant sample is not accounted for in this model and beyond the scope of this study. But it is noted, that for considering thermal diffusion only through a single aluminum particle, the characteristic evaporation time assuming a continuum droplet evaporation model was calculated to be on the order of $4.6 \times 10^6 d^2$ where d is

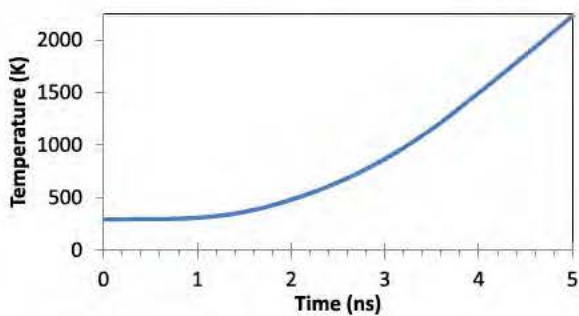


Fig. 7. Temperature of Al particle from joule heating COMSOL model.

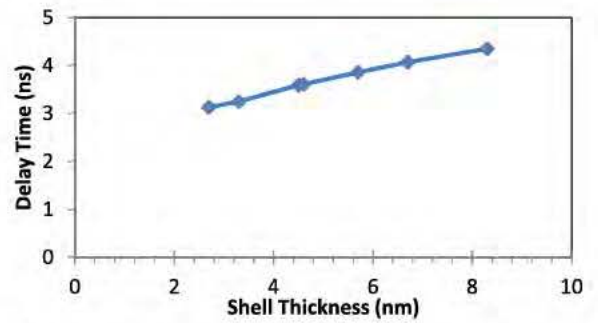


Fig. 8. Predicted ignition delay for a single Al particle with varying alumina shell thicknesses.

the aluminum particle diameter [12]. In this model applied to the particles studied here, the characteristic thermal evaporation time is approximately 50 ns, and greater than the joule heating times determined here. Instead, the trend in behavior as shell thickness is varied is of interest and can be correlated to ignition delay times.

Fig. 8 shows the ignition delay of the Al particles for all the Al₂O₃ shell thicknesses predicted by the COMSOL model.

The model shows that the ignition delay increases as the shell thickness increases. This result is consistent with the measured delay (Fig. 5) and implies that the increase in shell thickness retards thermal energy buildup within a single particle such that ignition delay times are extended. This result implies that joule heating is an Al ignition mechanism for electric stimuli.

The electrical conductivity was also measured using a high resistance low conductance meter and a two point probe method [6]. Fig. 9 shows that electrical conductivity decreases as shell thickness increases.

As the percent of Al₂O₃ increases, the electrical conductivity decreases. Also, as the percent of Al₂O₃ content increases, the electrical resistance increases and the current decreases, with a constant voltage. With more resistance impeding the flow of electric energy, joule heating of the aluminum core may be delayed thereby requiring more time to reach Al melting temperature and ignition.

4. Discussion

These results show that all Al + MoO₃ samples were ESD ignition sensitive (Fig. 5) but their sensitivity is controlled by the shell thickness surrounding the Al particle. Increasing shell thickness from 2.7 to 8.3 nm increases the ignition delay time up to 4 ms and requires up to 1000 V more electric input to achieve ignition (Figs. 5 and 6). Modeling the heat transfer through a single Al particle subjected to similar electric input conditions reveals a comparable

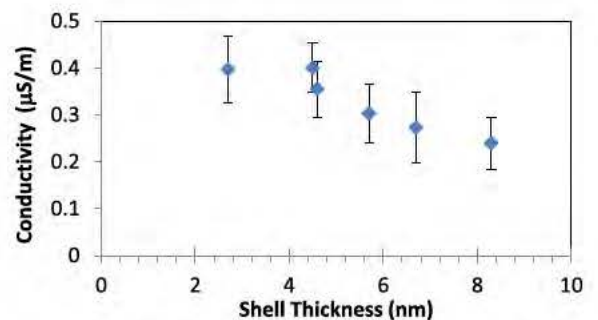


Fig. 9. Electrical conductivity of Al + MoO₃ powders with a varying Al₂O₃ shell thickness.

trend observed experimentally: increasing shell thickness leads to increasing ignition delay time and decreasing electrical conductivity (Figs. 8 and 9). Alumina retards energy propagation in the core–shell structure of the aluminum–alumina particle and this is represented by the COMSOL model (Figs. 7 and 8). This finding also suggests that joule heating is the primary mechanism of ignition for ESD stimuli.

5. Conclusion

Aluminum particles were synthesized with varying oxide shell thicknesses that ranged between 2.7 nm and 8.3 nm. Electrostatic discharge was used to ignite Al + MoO₃ and the ignition delay time was measured. The physics were also modeled using COMSOL Multiphysics software to approximate the temperature increase of an Al particle due to joule heating. The measured and modeled results both show similar trends in that the ignition delay increased as the Al₂O₃ shell thickness increased. The increase in ignition delay time suggests that the ESD ignition mechanism is joule heating because the model calculates transient temperatures based on transforming electrical stimuli into thermal energy. Alumina retards energy buildup within the particle such that thicker alumina shells result in longer ignition delay times. The results reveal that the current flow through the particle is a controlling parameter for ignition and a thicker shell increases resistance and therefore lowers the amount of current flowing through the aluminum core.

Acknowledgments

The authors M. Pantoya and E. Collins are grateful for support from the Army Research Office contract number W911NF 11 1 0439 and encouragement from our program manager, Dr. Ralph

Anthenien. Idaho National Laboratory is also gratefully acknowledged for supporting this collaborative work with internal funds via the LDRD program.

References

- [1] T.S. Ward, M.A. Trunov, M. Schoenitz, E.L. Dreizin, Experimental methodology and heat transfer model for identification of ignition kinetics of powdered fuels, *Int. J. Heat Mass Transfer* 49 (25–26) (Dec. 2006) 4943–4954.
- [2] D. Spitzer, M. Comet, C. Baras, Energetic nano-materials: opportunities for enhanced performances, *J. Phys. Chem. Solids* 71 (2) (2010) 100–108.
- [3] J. Sun, M.L. Pantoya, S.L. Simon, Dependence of size and size distribution on reactivity of aluminum nanoparticles in reactions with oxygen and MoO₃, *Thermochim. Acta* 444 (2) (May 2006) 117–127.
- [4] R. Williams, E. Dreizin, E. Beloni, Ignition of metal powder layers of different thickness by electrostatic discharge, *J. Propulsion Power* 28 (1) (2012) 132–139.
- [5] J.A. Puszynski, C.J. Bulian, J.J. Swiatkiewicz, Processing and ignition characteristics of aluminum–bismuth trioxide nanothermite system, *J. Propulsion Power* 23 (4) (Jul. 2007) 698–706.
- [6] C. Weir, M.L. Pantoya, G. Ramachandran, T. Dallas, D. Prentice, M. Daniels, Electrostatic discharge sensitivity and electrical conductivity of composite energetic materials, *J. Electrostat.* 71 (1) (Feb. 2012) 77–83.
- [7] M. Glor, Hazards due to electrostatic charging of powders, *J. Electrostat.* 16 (1985) 175–191.
- [8] T. Foley, A. Pacheco, J. Malchi, R. Yetter, K. Higa, Development of nanothermite composites with variable electrostatic discharge ignition thresholds, *Propel. Explos. Pyrotech.* 6 (6) (2007).
- [9] C.M. Weir, M.L. Pantoya, M.A. Daniels, The role of aluminum particle size in electrostatic ignition sensitivity of composite energetic materials, *Combust. Flame* 160 (May 2013) 2279–2281.
- [10] J. Granier, M. Pantoya, Laser ignition of nanocomposite thermites, *Combust. Flame* 138 (4) (Sep. 2004) 373–383.
- [11] K.T. Sullivan, N.W. Piekielek, C. Wu, S. Chowdhury, S.T. Kelly, T.C. Hufnagel, K. Fezzaa, M.R. Zachariah, Reactive sintering: an important component in the combustion of nanocomposite thermites, *Combust. Flame* 159 (1) (Jan. 2012) 2–15.
- [12] B. Dikici, M.L. Pantoya, V. Levitas, The effect of pre-heating on flame propagation behavior in nanocomposite thermites, *Combust. Flame* 157 (8) (2010) 1581–1585.